Influence of desert dust intrusions on ground-based and satellite-derived ultraviolet irradiance in southeastern Spain

M. Antón,[1] A. Valenzuela,[2,3] R. Román,[4] H. Lyamani,[2,3] N. Krotkov,[5] A. Arola,[6] F. J. Olmo,[2,3] and L. Alados-Arboledas[2,3]

Received 8 May 2012; revised 30 August 2012; accepted 6 September 2012; published 9 October 2012.

[1] The desert dust aerosols strongly affect propagation of solar radiation through the atmosphere, reducing surface irradiance available for photochemistry and photosynthesis. This paper evaluates effects of desert dust on surface UV erythemal irradiance (UVER), as measured by a ground-based broadband UV radiometer and retrieved from the satellite Ozone Monitoring Instrument (OMI) at Granada (southern Spain) from January 2006 to December 2010. The dust effects are characterized by the transmittance ratio of the measured UVER to the corresponding modeled clear sky value. The transmittance has an exponential dependency on aerosol optical depth (AOD), with minimum values of ~0.6 (attenuation of ~40%). The OMI UVER algorithm does not account for UV aerosol absorption, which results in overestimation of the ground-based UVER especially during dust episodes with a mean relative difference up to 40%. The application of aerosol absorption post-correction method reduces OMI bias up to ~13%. The results highlight great effect of desert dust on the surface UV irradiance in regions like southern Spain, where dust intrusions from Sahara region are very frequent.

Citation: Antón, M., A. Valenzuela, R. Román, H. Lyamani, N. Krotkov, A. Arola, F. J. Olmo, and L. Alados-Arboledas (2012), Influence of desert dust intrusions on ground-based and satellite-derived ultraviolet irradiance in southeastern Spain, *J. Geophys. Res.*, *117*, D19209, doi:10.1029/2012JD018056.

1. Introduction

[2] Mineral dust aerosol plays an important role in Earth's climate system, absorbing solar and thermal radiation and modulating Earth's radiative budget. The main sources of mineral dust are the desert areas, with the Sahara being the most important source in the northern hemisphere [*Prospero et al.*, 2002; *Ginoux et al.*, 2004; *Papayannis et al.*, 2005; *Liu et al.*, 2008]. Air masses loaded with Saharan dust particles frequently reach Spanish and Portuguese regions. Several studies analyzed Saharan dust contribution to ambient levels of suspended particulate matter, studying the synoptic meteorological conditions responsible for the transport of the dust air masses [*Rodríguez et al.*, 2001; *Escudero et al.*, 2005, 2006; *Querol et al.*, 2009]. Other studies focused on the retrievals of micro-physical and optical properties of Saharan dust using passive remote sensing measurements with sun-sky photometers [*Alados-Arboledas et al.*, 2003, 2008; *Lyamani et al.*, 2004, 2005, 2010; *Elias et al.*, 2006; *Toledano et al.*, 2007; *Cachorro et al.*, 2008; *Prats et al.*, 2008; *Wagner et al.*, 2009; *Valenzuela et al.*, 2012a, 2012b]. Lidar systems have also been used to characterize the vertical profile and structure of desert dust plumes [*Pérez et al.*, 2006; *Guerrero-Rascado et al.*, 2008, 2009; *Córdoba-Jabonero et al.*, 2011; *Preißler et al.*, 2011].

[3] However, there are relatively few studies analyzing effects of dust intrusions on shortwave solar radiation reaching the Earth's surface. [*Díaz et al.*, 2001; *Lyamani et al.*, 2006; *Santos et al.*, 2008; *Cachorro et al.*, 2008; *Antón et al.*, 2012a]. To our knowledge, only *Díaz et al.* [2007] and *Antón et al.* [2012b] have analyzed the atmospheric aerosol effects on spectral UV irradiance during two Saharan dust events in South Spain. In general, there are only a few works about this subject in literature [e.g., *di Sarra et al.*, 2002; *Meloni et al.*, 2003; *Kalashnikova et al.*, 2007; *García et al.*, 2009] due to the scarcity of routinely operational ground-based stations with high-quality instrumentation to measure simultaneously UV irradiance and aerosol data during desert dust intrusions.

[4] The analysis of the diverse atmospheric factors affecting the UV irradiance is motivated by the harmful effects of this radiation on human health, ecosystems, and materials [*Diffey*, 1991, 2004]. This paper focuses on the analysis of the influence of desert dust aerosol on the UV erythemally weighted surface irradiance (UVER) measured at Granada, a non-industrialized medium-sized city in

[1]Departamento de Física, Universidad de Extremadura, Badajoz, Spain.
[2]Departamento de Física Aplicada, Universidad de Granada, Granada, Spain.
[3]Centro Andaluz de Medio Ambiente, Universidad de Granada, Granada, Spain.
[4]Departamento de Física Aplicada, Universidad de Valladolid, Valladolid, Spain.
[5]Laboratory of Atmospheric Chemistry and Dynamics, NASA Goddard Space Flight Center, Greenbelt, Maryland, USA.
[6]Finnish Meteorological Institute, Kuopio, Finland.

Corresponding author: M. Antón, Departamento de Física, Universidad de Extremadura, ES-06071 Badajoz, Spain. (mananton@unex.es)

0148-0227/12/2012JD018056

southeastern Spain. The study analyzes desert dust intrusions detected during a period from January 2006 to December 2010 to evaluate the differences between the UVER measurements and the satellite retrievals from Ozone Monitoring Instrument (OMI) on NASA EOS Aura satellite [*Tanskanen et al.*, 2007]. Previously, largest differences between the satellite and ground-based UV irradiance data were reported in urban polluted areas, with elevated levels of UV-absorbing aerosols [*McKenzie et al.*, 2001; *Kazantzidis et al.*, 2006; *Tanskanen et al.*, 2007; *Ialongo et al.*, 2008; *Buchard et al.*, 2008]. Thus, it is expected that desert dust particles (with significant absorption in the UV spectral range) will also produce large differences between the satellite-derived and surface measured UV irradiance [e.g., *Antón et al.*, 2012b].

[5] The article has been organized as follows: Section 2 describes the instruments and data used in this study. Section 3 explains methodology. Section 4 discusses results and section 5 summarizes main conclusions.

2. Instruments and Data

2.1. Ground-Based Measurements

[6] The experimental data used in this study have been collected at the radiometric station located on the rooftop of the Andalusian Center for Environmental Studies (CEAMA, 37.17°N, 3.61°W, 680 m a.s.l.) in Granada, southeastern Spain. This station is operated by the Atmospheric Physics Group (GFAT) of the Granada University.

[7] A broadband UV radiometer, model UVB-1, manufactured by Yankee Environmental Systems, Inc. (Massachusetts, U.S.), measures spectrally integrated UV irradiance weighted with the erythemal action spectrum adopted by the Commission Internationale de l'Eclairage (CIE) [*McKinlay and Diffey*, 1987] (denoted as UVER). Measurements were sampled every ten seconds and recorded as one minute mean voltages on Campbell CR10X data acquisition systems. Output voltages are converted into UVER values applying the calibration factors derived from two calibration campaigns of broadband UV radiometers at the "El Arenosillo" INTA station in Huelva (Spain) in September 2007 and June 2011 [*Vilaplana et al.*, 2009]. These calibrations included spectral and angular characterization of the instruments and their absolute calibration, performed through the outdoor intercomparison with a reference Brewer spectroradiometer. Output voltages recorded by the UVB-1 radiometer were converted to UVER data applying conversion factors obtained from the "two-steps" calibration method [*Seckmeyer et al.*, 1997; *Webb et al.*, 2006]. *Antón et al.* [2011a] compared the UVER data provided by the UVB-1 radiometer installed in Granada with radiative transfer model calculations for a cloudless sky; their results have shown high quality of the UVER data used in this paper.

[8] The ground-based station is also equipped with a CM-11 pyranometer for measurements of global solar irradiance from 0.305 to 2.8 μm. This instrument is fully compliant with the highest ISO performance criteria with estimated relative uncertainty better than 2% [*Kratzenberg et al.*, 2006]. The stability of the pyranometer's calibration has been periodically verified using a reference CM-11 instrument located at the study station and used only for inter-comparison purposes. The calibration factors showed variations below 1% (four inter-comparisons performed between March 2005 and June 2010) which guarantees the stability of the global solar irradiance data used in this work.

[9] A Cimel CE-318 Sun photometer, co-located with the UVB-1 and CM-11 instruments, makes direct sun measurements with a 1.2° full field of view at seven wavelengths between 340 and 1020 nm, at every 15 min. This instrument is part of the Iberian network for Sun photometer aerosol measurements (RIMA), a scientific regional network federated to NASA AERONET global network [*Holben et al.*, 1998]. From the direct sun measurements and using the calibration constants provided by AERONET-RIMA, the aerosol optical depths (AOD) at seven wavelengths are derived following the method described in the works of *Alados-Arboledas et al.* [2003, 2008]. Furthermore, the inversion procedure of *Olmo et al.* [2006, 2008] is utilized to retrieve columnar aerosol optical and microphysical properties such as single scattering albedo (SSA). This inversion code uses as input parameters AOD data derived from direct Sun photometer measurements, and sky radiance measurements in the principal plane configuration.

2.2. Satellite Data

[10] The OMI satellite instrument is on board NASA EOS/Aura platform launched in July 2004 [*Schoeberl et al.*, 2006]. This instrument consists of a nadir viewing push-broom spectrometer that measures solar backscattered radiation in the spectral range from 270 nm to 500 nm with a resolution of 0.55 nm in the ultraviolet and 0.63 nm in the visible. The OMI instrument has a 2600 km wide viewing swath and it is capable of daily global contiguous mapping. The footprint size of satellite pixel is 13 by 24 km at nadir increasing up to ~150 km off-nadir viewing directions.

[11] The OMI surface UV algorithm (OMUVB) is based on the UV algorithm for Total Ozone Mapping Spectrometer (TOMS) instruments developed at NASA Goddard Space Flight Center (GSFC) [*Krotkov et al.*, 1998, 2001]. This algorithm estimates surface UV irradiance from lookup tables (LUTs) obtained by a radiative transfer model using the OMI-derived total ozone, surface albedo and cloud information as input parameters [*Tanskanen et al.*, 2006, 2007].

[12] In this study, the OMUVB product used is OPEDRate (Overpass Erythemal Dose Rate). In addition, OMUVB data set contains the Lambertian Equivalent Reflectivity (LER) at 360 nm which is used for cloud characterization. Additionally, we use the Aerosol Index (AI) calculated from 331 nm and 360 nm radiances which gives information about absorbing aerosols. All these OMI products are downloaded from the Aura Validation data Center site at http://avdc.gsfc.nasa.gov for the OMI station overpass data.

3. Methodology

[13] The inventory of Saharan desert dust events occurred at Granada from 2006 to 2010 is based on a published methodology using synthetic information from models, back-trajectories analysis, synoptic meteorological charts, satellite retrievals and surface data. Detailed information about this inventory can be found in the works of *Valenzuela et al.* [2012a, 2012b] who evaluated Saharan dust aerosol optical properties and its dependence on source region and transport pathways.

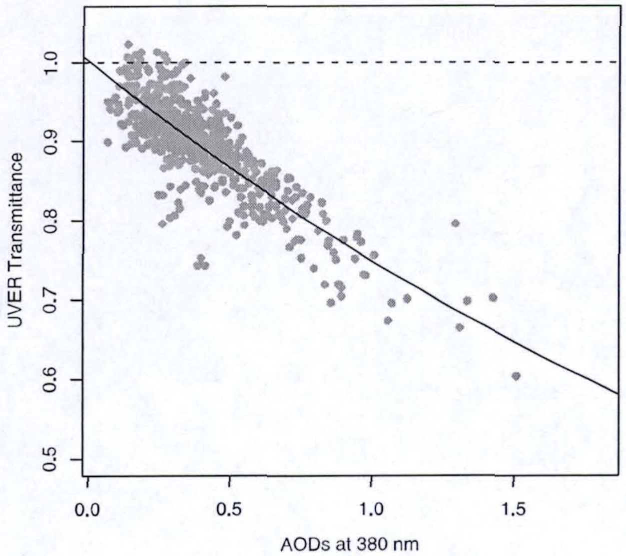

Figure 1. Atmospheric transmittance in the UV erythemal spectral range as a function of aerosol optical depth at 380 nm in the slant path (AODs) for solar zenith angles smaller than 60°. The solid exponential curve represents the values given by equation (3).

[14] In this work, the dust effect on the UVER is described in terms of the relative aerosol transmittance (T_{UVER}), relative to no-aerosol clear sky $UNER^0$ [*Krotkov et al.*, 1998]:

$$T_{UVER} = \frac{UVER}{UVER^0} \quad (1)$$

In this expression UVER represents the erythemal measurements recorded during desert dust intrusions, and $UVER^0$ corresponds to the erythemal data for the same solar zenith angle (SZA) estimated from the empirical expression [*Madronich*, 2007]:

$$\mathrm{UVER}^0 = a\ (\mu_0)^b \left(\frac{\mathrm{TOC}}{300}\right)^c \quad (2)$$

where μ_0 is the cosine of the SZA and TOC is the total ozone column in Dobson Units (DU) provided by the OMI satellite instrument (OMTO3 product using NASA TOMS V8 retrieval algorithm [*Bhartia and Wellemeyer*, 2002]). This parameterized radiative model can be adjusted using available experimental data, at the local site [*Koepke et al.*, 1998]. *Antón et al.* [2011b] calculated the coefficients (a, b and c) in equation (2) for Granada site using UVER measurements during cleanest air conditions at the site. They validated this empirical model using measurements collected during a period not previously used for calculating fitting coefficients. The results show a reliability of the empirical model (2), which estimates $UVER^0$ with a mean absolute bias less than 2.5%.

[15] Finally, the atmospheric aerosol transmittance is calculated from equation (1) by using measured UVER values averaged within ±2 min of each Cimel AOD retrieval during desert dust events (2006–2010).

[16] In order to analyze the effects of desert dust events on OMI-derived surface UV irradiances a single OMI ground pixel most closely collocated with Granada station is selected as the best match for each day. We used OMI pixels with centers from 1 km to 78 km from the study site, with the mean and median values being 17 and 11 km, respectively. Five surface UVER measurements within ±2 min from the OMI overpass at ~13:30 are averaged for comparison with the OMI data. Additionally, aerosol information derived from Cimel Sun photometer is averaged between 12:30 and 14:30 solar time on each day.

4. Results and Discussion

4.1. Effects on Ground-Based Measurements

[17] The mean value (±1 standard deviation) of the atmospheric aerosol transmittance (equation (1)) is 0.89 ± 0.06 or 11% average UVER reduction during desert dust intrusions over Granada. In ~12% dust cases UVER decreases more than 20% (T_{UVER} < 0.8), which represents significant reduction in UVER due to aerosol absorption [*Krotkov et al.*, 1998].

[18] Experimental studies about the evaluation of atmospheric transmittance in the UV range associated with desert dust episodes are very scarce: *Díaz et al.* [2007] reported atmospheric transmittance values between 0.92 and 0.95 for global UV irradiance (280–363 nm) measurements in southeastern Spain and *Kalashnikova et al.* [2007] evaluated the atmospheric transmittance at 340–380 nm during 2 dust events in Australia, showing values larger than 0.90. These studies are focused on specific short-term dust events, while our study is based on a long-term inventory of dust episodes. Figure 1 shows measured UVER transmittance (T_{UVER}) as a function of AOD at 380 nm in the slant path (AOD_s) for solar zenith angles (SZA) less than 60°. This variable takes into account the aerosol extinction in the slant column and it is derived by multiplying AOD with the air mass factor equal to sec(SZA) for each measurement [*García et al.*, 2006; *Kazadzis et al.*, 2009]. From this figure, it can be seen that T_{UVER} decreases as AOD_s increases, with minimum T_{UVER} values around 0.6 for AOD_s of 1.5 (attenuation of ~40%) which highlights great influence of desert dust on measured UVER values.

[19] The T_{UVER} dependence on AOD can be parameterized as the exponential expression:

$$T_{UVER} = \exp(-k \cdot AOD_s) \quad (3)$$

where k depends on aerosol single scattering co-albedo, 1-ω [*Krotkov et al.*, 1998]. This parameter has been derived from the lineal regression analysis between the logarithm of T_{UVER} and AODs, resulting in a mean value of 0.291 ± 0.008 ($R^2 \sim 0.7$). Corresponding curve is shown in Figure 1.

[20] *Krotkov et al.* [1998] used a radiative transfer model to obtain the parameter k for different aerosol models. For non-absorbing aerosol (e.g., anthropogenic sulfate), they showed k values less than 0.15. Such small k values (i.e., T_{UVER} ~ 1–2% for AOD = 0.1) are explained by the mutually compensating effects between the reduction of the direct flux by aerosol extinction and corresponding increase of the diffuse flux by aerosol scattering. For two dust

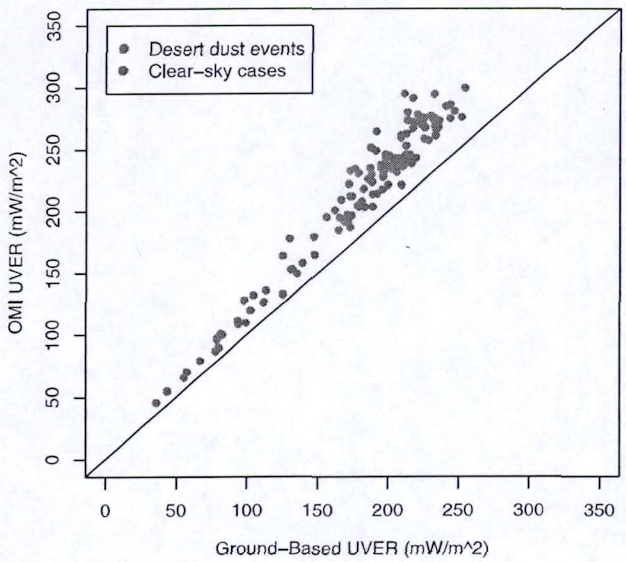

Figure 2. Correlation between OMI and ground-based UVER data for desert dust cases under cloud-free satellite pixels (in red). Subset of data for pristine (clear-sky) cases under cloud- and aerosol-free conditions are shown in gray. The study period is between January 2006 and December 2010. The solid black line is the zero bias line, unit slope.

models, the authors showed that the k values are substantially higher (between 0.3 and 0.6 for more absorbing dust). The larger k values can be explained by strong absorption of UV radiation by the mineral compounds of the desert dust such as hematite and goethite [*Horvath*, 1993; *Alfaro et al.*, 2004]. The lower k $\sim$ 0.3 value reported in our work compared to *Krotkov et al.* [1998] simulations can be explained by the location of our site thousand kilometers away from the desert dust source. Long-range transport of desert dust results in aging and mixing with other aerosol types leading to modification of its optical properties [*Bauer et al.*, 2011]. Recently, *Rodríguez et al.* [2011] have shown that anthropogenic emissions from crude oil refineries and power plants, located in North African industrial areas, contribute to desert dust mixing with other type of particles.

4.2. Dust Effects on Satellite Data

[21] OMI surface UV algorithm assumes that clouds and aerosols are non-absorbing and, therefore, the satellite-derived surface UV irradiances are expected to show overestimation for regions that are affected by absorbing aerosols such as smoke or desert dust [*Tanskanen et al.*, 2007].

[22] The variability of cloudiness within the OMI pixel (13 by 24 km for nadir viewing) can lead to significant difference between ground-based and satellite derived UVER data [*Weihs et al.*, 2008; *Antón et al.*, 2010]. To study the influence of desert dust aerosols on OMI UVER data, predominantly cloud-free pixels should be considered in the analysis. We use OMI measured Lambertian Equivalent reflectivity (LER) values as proxy for cloud contaminated OMI scenes [*Krotkov et al.*, 2001]. Specifically, we reject satellite scenes with LER values larger than 0.1 [*Kalliskota et al.*, 2000]. Figure 2 shows the relationship between OMI retrieved and measured UVER data for desert dust events detected at Granada under cloud-free conditions (LER < 0.1). The number of cloud-free days analyzed is 75 (69% of all dusty days). It can be seen that the correlation between satellite and ground-based UVER data is good ($R^2 \sim 0.95$), but a strong bias is also evident. The mean bias error (MBE) calculated as the average of the relative differences between OMI and measured UVER data ($UVER^{OMI}$-$UVER^{EXP}$/ $UVER^{EXP}$) is +22 $\pm$ 7% (OMI data being higher) where the uncertainty is characterized by the BE standard deviation.

[23] In order to evaluate what part of this large OMI bias can be attributed to the presence of desert dust particles, the relationship between OMI and ground-based UVER data is analyzed for dust-free and cloud-free (i.e., pristine) conditions, which we call "clear sky." Three different criteria are simultaneously applied for selecting clear sky cases. First, LER values smaller than 0.1 allow identify cloud-free satellite pixels. Second, the clearness index (k_t) was used to characterize the atmospheric turbidity during satellite overpass. The index is obtained from the ratio of the global solar irradiance to the extraterrestrial global solar irradiance on a horizontal surface [*Alados-Arboledas et al.*, 2000]. In order to select cases with low turbidity, a conservative threshold of k_t equal to 0.75 was chosen instead of the value of 0.65 used by other authors [e.g., *Kudish et al.*, 1983; *Udo*, 2000]. This higher threshold guarantees that the selected cases correspond to the cleanest air conditions that occur at Granada. The third criteria was to select those cases with AOD at 440 nm smaller than 0.1. Thus, we have implicitly assumed in this work that the atmospheric aerosol detected on clear-sky cases is the natural background. The pairs of satellite and ground-based UVER data recorded during clear-sky conditions are added to Figure 2. From this plot, it is highlighted that OMI bias is substantially reduced during satellite overpass under clear-sky conditions. Thus, the MBE decreases to (+14.2 $\pm$ 4.1)% for these clear cases. On average, desert dust intrusions over Granada cause an increase of the OMI bias by additional 8 percentage points which is mainly related to the fact that current OMUVB algorithm assumes no absorbing aerosols [*Tanskanen et al.*, 2007]. The main result of this assumption is the UVER overestimation due to the neglected aerosol absorption. In addition, since desert dust particles also reduce backscatter radiation reaching the satellite, the OMI algorithm underestimates the effective cloud optical depth which produces an additional overestimation in UV radiation products [*Krotkov et al.*, 1998, 2001]. This effective cloud optical depth is derived from matching the measured 360 nm radiance at the OMI overpass time with the modeled radiance assuming non-absorbing C1 cloud layer [*Krotkov et al.*, 2001]. Nevertheless, we would like to point out that the analysis for clear-sky conditions shows a residual positive OMI bias around 14% which is not due to aerosol absorption, but can be related to several sources of uncertainty both in satellite and ground-based data.

[24] Several papers [e.g., *Krotkov et al.*, 2005; *Arola et al.*, 2005, 2009; *Ialongo et al.*, 2008; *Kazadzis et al.*, 2009; *Cachorro et al.*, 2010] have used the column aerosol absorption optical depth (AAOD) to quantify the error in the OMI UVER product due to the omission of correction for absorbing aerosols in the current OMI UV algorithm. This variable is calculated from the following expression:

$$AAOD(\lambda) = AOD(\lambda) \cdot [1 - SSA(\lambda)], \quad (4)$$

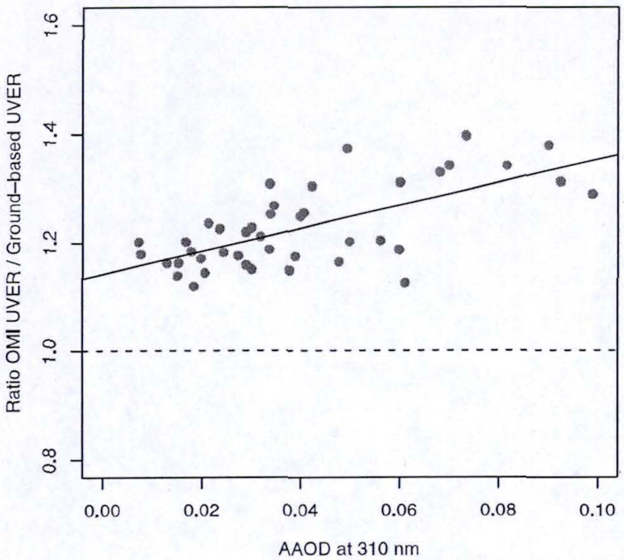

Figure 3. Ratio of OMI to ground-based UVER data as a function of the aerosol absorption optical depth (AAOD) extrapolated to 310 nm from Cimel values at 440 nm and 870 nm using Absorbing Angstrom Exponent for desert dust cases detected between January 2006 and December 2008. The solid line represents the regression line, with the slope of the fit b = 2.69 (b parameter in equation (6)).

where SSA is the single scattering albedo which can be retrieved from the sky radiance measured by the Cimel Sun photometer at 440, 675, 870 and 1020 nm [*Olmo et al.*, 2006, 2008] or direct to diffuse irradiance ratio measured by UV-MFRSR [*Krotkov et al.*, 2005].

[25] For the OMI bias correction it is necessary to obtain the AAOD at UV wavelengths that are not currently measured with Cimel data. In order to estimate AAOD at 310 nm, we use the following power law wavelength dependence [*Bergstrom et al.*, 2007]:

$$AAOD(\lambda) = c\cdot\lambda^{-AAE}, \qquad (5)$$

where AAE is the Absorption Angstrom Exponent which has been derived from the AAOD at 440 and 870 nm.

[26] Figure 3 shows the ratios of OMI to ground-based UVER data plotted against AAOD at 310 nm estimated using equation (5). All dusty cloud-free data recorded for the period January 2006–December 2008 are included in this plot. It can be noticed that the ratio increases with increasing AAOD, confirming that dust aerosol absorption can partially explain positive OMI UVER bias found in the satellite-ground-based comparison. The regression analysis provides a slope of the fit of 2.1 ± 0.4, indicating the way in which the OMI bias increases with an increasing amount of aerosol absorption. Additionally, the linear least squares fit shows an intercept value of 1.14 ± 0.02 which corresponds to the remaining bias under pristine cloud- and aerosol-free conditions. This value suggests that OMI UVER data are biased 14% high compared to the ground-based measurements for clear sky cases.

[27] Based on the above results, OMI UVER data can be post-corrected using the expression proposed by *Krotkov et al.* [2005]:

$$UVER^{OMI}_{corr} = \frac{UVER^{OMI}_{operational}}{(1 + b\cdot AAOD)}, \qquad (6)$$

where the denominator accounts for the presence of absorbing aerosols during OMI overpass time, with b being the slope of the regression analysis performed in the previous paragraph.

[28] Figure 4 shows the relationship between the reference ground-based UVER measurements and corrected OMI data for an independent data set corresponding to the period January 2009–December 2010 (not previously used for calculating the b parameter). It can be seen that correction method produces a clear reduction of the OMI bias. Thus, the MBE decreases from (+21 ± 5)% for operational satellite data to (+13 ± 4)% for corrected data, slightly smaller than the bias obtained for clear sky conditions (14%) which shows the level of improvement that may be reached with the off-line correction methodology.

[29] For the off-line aerosol correction of the OMI UV data, *Arola et al.* [2009] used the equation (6) with b parameter equal to 3 and monthly AAOD values from the global aerosol climatology of *Kinne* [2009]. The improvement in the OMI UV that can be achieved with this correction has been also evaluated by comparing with experimental UVER data recorded at Granada for the period January 2009–December 2010. The MBE (+13 ± 5)% is close to the bias obtained with the correction method used in our work, but with a larger standard deviation. Therefore, the Arola's correction method could be successfully applied to post correct operational OMI UV products over geographical

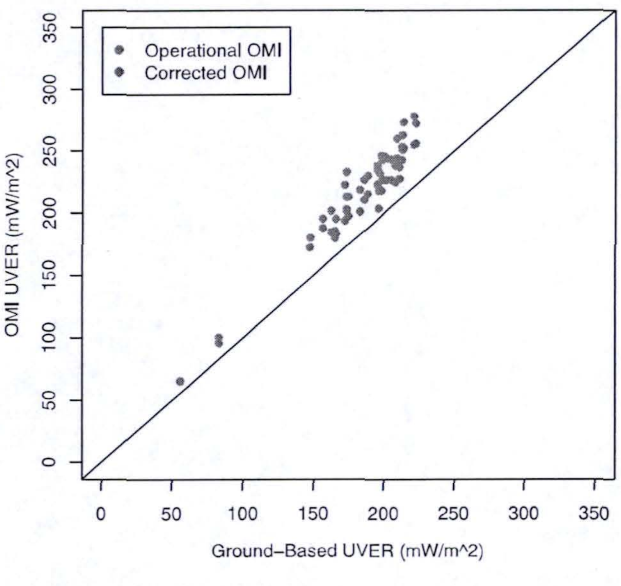

Figure 4. Correlation between OMI and ground-based UVER data for evaluation data set: desert dust cases detected between January 2009 and December 2010. Operational satellite data are in red and corrected satellite data in gray. The solid black line is the zero bias line, unit slope.

regions where experimental aerosol measurements are not available. This correction is expected to be implemented in the next re-processing of the OMI data set.

[30] The predecessor of the satellite OMI instrument was the TOMS instrument whose archived UV products were in fact corrected for aerosol absorption effects (dust and carbonaceous particles) [*Krotkov et al.*, 1998]. This correction was applied for those aerosol cases, identified from the TOMS measurements: a combination of the Aerosol Index (AI) larger than 0.5 and the LER less than 0.15. Thus, the AI = 0.5 is the threshold value chosen by TOMS UV algorithm to distinguish between absorbing and non-absorbing aerosol in the free troposphere. Contrary to the TOMS UV products, the current surface UV OMI algorithm does not use any correction for absorbing aerosols [*Tanskanen et al.*, 2007]. For the 75 dusty cloud-free days selected in our work, the AI given by OMI is larger than 0.5 in 56 days (75%) which indicate that this satellite product may provide better information about the absorbing properties of the aerosol load in each pixel. However, the ratio satellite/ground-based UVER data presents a poor correlation with AI values (plot not shown) suggesting that AI itself is not the best quantity to evaluate the effect of absorbing aerosols on the OMI UV bias. It is better using AAOD (equation (4)) estimated from models [*Arola et al.*, 2009] or ground measurements [*Krotkov et al.*, 2005].

5. Conclusions

[31] A long inventory of Sahara desert dust events recorded at Granada (Spain) has been used to analyze the influence of this type of particles on broadband surface UV irradiance weighted by erythemal action spectrum (UVER) as retrieved by satellite (OMI) and measured by ground-based instruments.

[32] The presence of desert dust aerosols over the study site causes average reductions of the UVER by about 11% with respect to clear-sky conditions. Reductions larger than 20% are found in 12.5% of all desert cases. These results reveal that the desert dust particles markedly affect the propagation of the UV radiation through the atmosphere.

[33] The UVER data derived from the OMI satellite instrument are biased high compared the ground-based UVER measurements during the desert dust cases with a mean relative difference of 22%. The analysis of pristine, clear-sky cases shows that 8% of the bias can be attributed to the fact that current OMI UV algorithm assumes no absorbing aerosols. Therefore, the effect of desert dust events on the UV irradiance derived from the OMI instrument cannot be neglected for regions like southern Spain, where the intrusions of the desert dust are frequent.

[34] The aerosol absorption bias can be corrected off-line. The post-correction has been tested using an independent data set and resulted in reduction of the bias from ~21% for operational satellite UVER data to ~13% for corrected data. The remaining positive bias (OMI being higher), indicate additional sources for discrepancy.

[35] Thus, OMI -derived UVER data have been shown to be overestimated in locations affected by desert dust. Therefore, reliable estimates of UV in these locations are dependent on the availability of quality assured ground-based measurements.

[36] **Acknowledgments.** Manuel Antón thanks Ministerio de Ciencia e Innovación and Fondo Social Europeo for the award of a postdoctoral grant (Ramón y Cajal). This work was partially supported by the Andalusian Regional Government through projects P08-RNM-3568 and P10-RNM-6299, the Ministerio de Ciencia e Innovación through projects CGL2008-05939-C03-03/CLI, CGL2010-18782, CGL-2011-2992-1-C02-01 and CSD2007-00067, and by European Union through ACTRIS project (EU INFRA-2010-1.1.16-262254). Nickolay Krotkov acknowledges support from NASA Earth Science Division.

References

Alados-Arboledas, L., F. J. Olmo, I. Alados, and M. Pérez (2000), Parametric models to estimate photosynthetically active radiation in Spain, *Agric. For. Meteorol.*, *101*, 187–201, doi:10.1016/S0168-1923(99)00163-X.

Alados-Arboledas, L., H. Lyamani, and F. J. Olmo (2003), Aerosol size properties at Armilla, Granada (Spain), *Q. J. R. Meteorol. Soc.*, *129*, 1395–1413, doi:10.1256/qj.01.207.

Alados-Arboledas, L., et al. (2008), Aerosol columnar properties retrieved from CIMEL radiometers during VELETA 2002, *Atmos. Environ.*, *42*, 2654–2667, doi:10.1016/j.atmosenv.2007.10.006.

Alfaro, S. C., S. Lafon, J. L. Rajot, P. Formenti, A. Gaudichet, and M. Maille (2004), Iron oxides and light absorption by pure desert dust: An experimental study, *J. Geophys. Res.*, *109*, D08208, doi:10.1029/2003JD004374.

Antón, M., V. E. Cachorro, J. M. Vilaplana, C. Toledano, N. A. Krotkov, A. Arola, A. Serrano, and B. de la Morena (2010), Comparison of UV irradiances from Aura/Ozone Monitoring Instrument (OMI) with Brewer measurements at El Arenosillo (Spain)—Part 1: Analysis of parameter influence, *Atmos. Chem. Phys.*, *10*, 5979–5989, doi:10.5194/acp-10-5979-2010.

Antón, M., J. E. Gil, A. Cazorla, J. Fernández-Gálvez, J. M. Vilaplana, F. J. Olmo, and L. Alados-Arboledas (2011a), Influence of the calibration on experimental UV index at a midlatitude site, Granada (Spain), *Atmos. Meas. Tech.*, *4*, 499–507, doi:10.5194/amt-4-499-2011.

Antón, M., J. E. Gil, J. Fernández-Gálvez, H. Lyamani, A. Valenzuela, I. Foyo-Moreno, F. J. Olmo, and L. Alados-Arboledas (2011b), Evaluation of the aerosol forcing efficiency in the UV erythemal range at Granada, Spain, *J. Geophys. Res.*, *116*, D20214, doi:10.1029/2011JD016112.

Antón, M., A. Valenzuela, A. Cazorla, J. E. Gil, J. Fernández-Gálvez, H. Lyamani, I. Foyo-Moreno, F. J. Olmo, and L. Alados-Arboledas (2012a), Global and diffuse shortwave irradiance during a strong desert dust episode at Granada (Spain), *Atmos. Res.*, *118*, 232–239, doi:10.1016/j.atmosres.2012.07.007.

Antón, M., M. Sorribas, Y. Bennouna, J. M. Vilaplana, V. E. Cachorro, J. Gröbner, and L. Alados-Arboledas (2012b), Effects of an extreme desert dust event on the spectral ultraviolet irradiance at El Arenosillo (Spain), *J. Geophys. Res.*, *117*, D03205, doi:10.1029/2011JD016645.

Arola, A., S. Kazadzis, N. Krotkov, A. Bais, J. Gröbner, and J. R. Herman (2005), Assessment of TOMS UV bias due to absorbing aerosols, *J. Geophys. Res.*, *110*, D23211, doi:10.1029/2005JD005913.

Arola, A., S. Kazadzis, A. Lindfors, N. A. Krotkov, J. Kujanpä, and J. Tamminen (2009), A new approach to correct for absorbing aerosols in OMI UV, *Geophys. Res. Lett.*, *36*, L22805, doi:10.1029/2009GL041137.

Bauer, S., E. Bierwirth, M. Esselborn, A. Petzold, A. Macke, T. Trautmann, and M. Wendisch (2011), Airborne spectral radiation measurements to derive solar radiative forcing of Saharan dust mixed with biomass burning smoke particles, *Tellus, Ser. B*, *63*, 742–750.

Bergstrom, R. W., P. Pilewskie, P. B. Russell, J. Redemann, T. C. Bond, and P. K. Quinn (2007), Spectral absorption properties of atmospheric aerosols, *Atmos. Chem. Phys.*, *7*, 5937–5943, doi:10.5194/acp-7-5937-2007.

Bhartia, P. K., and C. Wellemeyer (2002), TOMS-V8 total O3 algorithm, in *OMI Algorithm Theoretical Basis Document*, vol. II, *OMI Ozone Products*, edited by P. K. Bhartia, pp. 15–31, NASA Goddard Space Flight Cent., Greenbelt, Md. [Available at http://eospso.gsfc.nasa.gov/eos_homepage/for_scientists/atbd/index.php]

Buchard, V., C. Brogniez, F. Auriol, B. Bonnel, J. Lenoble, A. Tanskanen, B. Bojkov, and P. Veefkind (2008), Comparison of OMI ozone and UV irradiance data with ground-based measurements at two French sites, *Atmos. Chem. Phys.*, *8*, 4517–4528, doi:10.5194/acp-8-4517-2008.

Cachorro, V. E., C. Toledano, N. Prats, M. Sorribas, S. Mogo, A. Berjón, B. Torres, R. Rodrigo, J. de la Rosa, and A. M. De Frutos (2008), The strongest desert dust intrusion mixed with smoke over the Iberian Peninsula registered with Sun photometry, *J. Geophys. Res.*, *113*, D14S04, doi:10.1029/2007JD009582.

Cachorro, V. E., C. Toledano, M. Antón, A. Berjón, A. de Frutos, A. Arola, and N. A. Krotkov (2010), Comparison of UV irradiances from Aura/Ozone Monitoring Instrument (OMI) with Brewer measurements at El

Arenosillo (Spain)—Part 2: Analysis of site aerosol influence, *Atmos. Chem. Phys.*, *10*, 11,867–11,880, doi:10.5194/acp-10-11867-2010.

Córdoba-Jabonero, C., et al. (2011), Synergetic monitoring of Saharan dust plumes and potential impact on surface: A case study of dust transport from Canary Islands to Iberian Peninsula, *Atmos. Chem. Phys.*, *11*, 3067–3091, doi:10.5194/acp-11-3067-2011.

Díaz, J. P., F. J. Expósito, C. J. Torres, F. Herrera, J. M. Prospero, and M. C. Romero (2001), Radiative properties of aerosols in Saharan dust outbreaks using ground-based and satellite data: Applications to radiative forcing, *J. Geophys. Res.*, *106*, 18,403–18,416, doi:10.1029/2001JD900020.

Díaz, A. M., et al. (2007), Aerosol radiative forcing efficiency in the UV region over southeastern Mediterranean: VELETA2002 campaign, *J. Geophys. Res.*, *112*, D06213, doi:10.1029/2006JD007348.

Diffey, B. (1991), Solar ultraviolet radiation effects on biological systems, *Phys. Med. Biol.*, *36*, 299–328, doi:10.1088/0031-9155/36/3/001.

Diffey, B. (2004), Climate change, ozone depletion and the impact on ultraviolet exposure of human skin, *Phys. Med. Biol.*, *49*, R1–R11, doi:10.1088/0031-9155/49/1/R01.

di Sarra, A., M. Cacciani, P. Chamard, C. Cornwall, J. J. DeLuisi, T. Di Iorio, P. Disterhoft, G. Fiocco, D. Fua, and F. Monteleone (2002), Effects of desert dust and ozone on the ultraviolet irradiance at the Mediterranean island of Lampedusa during PAUR II, *J. Geophys. Res.*, *107*(D18), 8135, doi:10.1029/2000JD000139.

Elias, T., A. M. Silva, N. Belo, S. Pereira, P. Formenti, G. Helas, and F. Wagner (2006), Aerosol extinction in a remote continental region of the Iberian Peninsula during summer, *J. Geophys. Res.*, *111*, D14204, doi:10.1029/2005JD006610.

Escudero, M., S. Castillo, X. Querol, A. Avila, M. Alarcón, M. M. Viana, A. Alastuey, E. Cuevas, and S. Rodríguez (2005), Wet and dry African dust episodes over eastern Spain, *J. Geophys. Res.*, *110*, D18S08, doi:10.1029/2004JD004731.

Escudero, M., A. Stein, R. R. Draxler, X. Querol, A. Alastuey, S. Castillo, and A. Avila (2006), Determination of the contribution of northern Africa dust source areas to PM10 concentrations over the central Iberian Peninsula using the Hybrid Single-Particle Lagrangian Integrated Trajectory model (HYSPLIT) model, *J. Geophys. Res.*, *111*, D06210, doi:10.1029/2005JD006395.

García, O. E., A. M. Díaz, F. J. Expósito, J. P. Díaz, J. Gröbner, and V. E. Fioletov (2006), Cloudless aerosol forcing efficiency in the UV region from AERONET and WOUDC databases, *Geophys. Res. Lett.*, *33*, L23803, doi:10.1029/2006GL026794.

García, O. E., A. M. Díaz, F. J. Expósito, and J. P. Díaz (2009), Aerosol radiative forcing and forcing efficiency in the UVB for regions affected by Saharan and Asian mineral dust, *J. Atmos. Sci.*, *66*, 1033–1040, doi:10.1175/2008JAS2816.1.

Ginoux, P., J. M. Prospero, O. Torres, and M. Chin (2004), Long-term simulation of global dust distribution with the GOCART model: Correlation with North Atlantic Oscillation, *Environ. Model. Softw.*, *19*(2), 113–128, doi:10.1016/S1364-8152(03)00114-2.

Guerrero-Rascado, J. L., B. Ruiz, and L. Alados-Arboledas (2008), Multispectral lidar characterization of the vertical structure of Saharan dust aerosol over southern Spain, *Atmos. Environ.*, *42*, 2668–2681, doi:10.1016/j.atmosenv.2007.12.062.

Guerrero-Rascado, J. L., F. J. Olmo, I. Avilés-Rodríguez, F. Navas-Guzmán, D. Pérez-Ramírez, H. Lyamani, and L. Alados Arboledas (2009), Extreme Saharan dust event over the southern Iberian Peninsula in September 2007: Active and passive remote sensing from surface and satellite, *Atmos. Chem. Phys.*, *9*, 8453–8469, doi:10.5194/acp-9-8453-2009.

Holben, B., et al. (1998), AERONET—A federated instrument network and data archive for aerosol characterization, *Remote Sens. Environ.*, *66*(1), 1–16, doi:10.1016/S0034-4257(98)00031-5.

Horvath, H. (1993), Atmospheric light absorption—A review, *Atmos. Environ.*, *27*, 293–317, doi:10.1016/0960-1686(93)90104-7.

Ialongo, I., G. R. Casale, and A. M. Siani (2008), Comparison of total ozone and erythemal UV data from OMI with ground-based measurements at Rome station, *Atmos. Chem. Phys.*, *8*, 3283–3289, doi:10.5194/acp-8-3283-2008.

Kalashnikova, O. V., F. P. Mills, A. Eldering, and D. Anderson (2007), Application of satellite and ground-based data to investigate the UV radiative effects of Australian aerosols, *Remote Sens. Environ.*, *107*, 65–80, doi:10.1016/j.rse.2006.07.025.

Kalliskota, S., J. Kaurola, P. Taalas, J. Herman, E. Celarier, and N. Krotkov (2000), Comparison of daily UV doses estimated from Nimbus 7/TOMS measurements and ground-based spectroradiometer data, *J. Geophys. Res.*, *105*, 5059–5067, doi:10.1029/1999JD900926.

Kazadzis, S., N. Kouremeti, A. Bais, A. Kazantzidis, and C. Meleti (2009), Aerosol forcing efficiency in the UVA region from spectral solar irradiance measurements at an urban environment, *Ann. Geophys.*, *27*, 2515–2522, doi:10.5194/angeo-27-2515-2009.

Kazantzidis, A., et al. (2006), Comparison of satellite-derived UV irradiances with ground-based measurements at four European stations, *J. Geophys. Res.*, *111*, D13207, doi:10.1029/2005JD006672.

Kinne, S. (2009), Climatologies of cloud related aerosols: Part 1: Particle number and size, in *Clouds in the Perturbed Climate System*, edited by J. Heintzenberg and R. J. Charlson, chap. 3, pp. 37–58, MIT Press, Cambridge, Mass.

Koepke, P., et al. (1998), Comparison of models used for UV index calculations, *Photochem. Photobiol.*, *67*, 657–662, doi:10.1111/j.1751-1097.1998.tb09109.x.

Kratzenberg, M. G., H. G. Beyer, S. Colle, and A. Albertazzi (2006), Uncertainty calculations in pyranometer measurements and application, paper presented at 2006 International Solar Energy Conference, Am. Soc. of Mech. Eng., Denver, Colo.

Krotkov, N. A., P. K. Barthia, J. R. Herman, V. Fioletov, and J. Kerr (1998), Satellite estimation of spectral surface UV irradiance in the presence of tropospheric aerosols, *J. Geophys. Res.*, *103*, 8779–8793, doi:10.1029/98JD00233.

Krotkov, N. A., J. R. Herman, P. K. Barthia, V. Fioletov, and Z. Ahmad (2001), Satellite estimation of spectral surface UV irradiance: 2. Effects of homogeneous clouds and snow, *J. Geophys. Res.*, *106*, 11,743–11,759, doi:10.1029/2000JD900721.

Krotkov, N. A., P. K. Barthia, J. R. Herman, J. Slusser, G. Scott, G. Labow, A. P. Vasilkov, T. F. Eck, O. Dubovik, and B. N. Holben (2005), Aerosol ultraviolet absorption experiment (2000 to 2004), part 2: Absorption optical thickness, refractive index, and single scattering albedo, *Opt. Eng.*, *44*(4), 041005, doi:10.1117/1.1886819.

Kudish, A., D. Wolf, and Y. Machalv (1983), Solar radiation data for Beer Sheva, Israel, *Sol. Energy*, *30*, 33–37, doi:10.1016/0038-092X(83)90003-8.

Liu, Z., et al. (2008), CALIPSO lidar observations of the optical properties of Saharan dust: A case study of long-range transport, *J. Geophys. Res.*, *113*, D07207, doi:10.1029/2007JD008878.

Lyamani, H., F. J. Olmo, and L. Alados-Arboledas (2004), Long-term changes in aerosol radiative properties at Armilla (Spain), *Atmos. Environ.*, *38*, 5935–5943, doi:10.1016/j.atmosenv.2004.07.021.

Lyamani, H., F. J. Olmo, and L. Alados-Arboledas (2005), Saharan dust outbreak over south-eastern Spain as detected by Sun photometer, *Atmos. Environ.*, *39*, 7276–7284.

Lyamani, H., F. J. Olmo, A. Alcántara, and L. Alados-Arboledas (2006), Atmospheric aerosols during the 2003 heat wave in southeastern Spain II: Microphysical columnar properties and radiative forcing, *Atmos. Environ.*, *39*, 7276–7284.

Lyamani, H., F. J. Olmo, and L. Alados-Arboledas (2010), Physical and optical properties of aerosols over an urban location in Spain: Seasonal and diurnal variability, *Atmos. Chem. Phys.*, *10*, 239–254, doi:10.5194/acp-10-239-2010.

Madronich, S. (2007), Analytic formula for the clear-sky UV index, *Photochem. Photobiol.*, *83*(6), 1537–1538, doi:10.1111/j.1751-1097.2007.00200.x.

McKenzie, R. L., G. Seckmeyer, A. F. Bais, J. B. Kerr, and S. Madronich (2001), Satellite retrievals of erythemal UV dose compared with ground-based measurements at northern and southern midlatitudes, *J. Geophys. Res.*, *106*, 24,051–24,062, doi:10.1029/2001JD000545.

McKinlay, A. F., and B. L. Diffey (1987), A reference spectrum for ultraviolet induced erythema in human skin, *CIE J.*, *6*, 21–27.

Meloni, D., F. Marenco, and A. di Sarra (2003), Ultraviolet radiation and aerosol monitoring at Lampedusa, Italy, *Ann. Geophys.*, *46*, 373–383.

Olmo, F. J., A. Quirantes, A. Alcantara, H. Lyamani, and L. Alados-Arboledas (2006), Preliminary results of a non-spherical aerosol method for the retrieval of the atmospheric aerosol optical properties, *J. Quant. Spectrosc. Radiat. Transfer*, *100*, 305–314, doi:10.1016/j.jqsrt.2005.11.047.

Olmo, F. J., A. Quirantes, V. Lara, H. Lyamani, and L. Alados-Arboledas (2008), Aerosol optical properties assessed by an inversion method using the solar principal plane for non-spherical particles, *J. Quant. Spectrosc. Radiat. Transfer*, *109*, 1504–1516, doi:10.1016/j.jqsrt.2007.12.019.

Papayannis, A., D. Balis, V. Amiridis, G. Chourdakis, G. Tsaknakis, C. Zerefos, A. D. Castanho, S. Nickovic, S. Kazadzis, and J. Grabowski (2005), Measurements of Saharan dust aerosols over the Eastern Mediterranean using elastic-Raman lidar, spectrophotometric and satellite observations in the frame of the EARLINET project, *Atmos. Chem. Phys.*, *5*, 2065–2079, doi:10.5194/acp-5-2065-2005.

Pérez, C., S. Nickovic, J. M. Baldasano, M. Sicard, F. Rocadenbosch, and V. E. Cachorro (2006), A long Saharan dust event over the western Mediterranean: Lidar, Sun photometer observations, and regional dust modeling, *J. Geophys. Res.*, *111*, D15214, doi:10.1029/2005JD006579.

Prats, N., V. E. Cachorro, M. Sorribasa, S. Mogo, A. Berjón, C. Toledano, A. M. de Frutos, J. de la Rosa, N. Laulainen, and B. A. de la Morena (2008), Columnar aerosol optical properties during "El Arenosillo 2004 summer campaign," *Atmos. Environ.*, *42*, 2643–2653, doi:10.1016/j.atmosenv.2007.07.041.

Preißler, J., F. Wagner, S. N. Pereira, and J. L. Guerrero-Rascado (2011), Multi-instrumental observation of an exceptionally strong Saharan dust outbreak over Portugal, *J. Geophys. Res.*, *116*, D24204, doi:10.1029/2011JD016527.

Prospero, J. M., P. Ginoux, O. Torres, S. E. Nicholson, and T. E. Gill (2002), Environmental characterization of global sources of atmospheric soil dust identified with the NIMBUS 7 Total Ozone Mapping Spectrometer (TOMS) absorbing aerosol product, *Rev. Geophys.*, *40*(1), 1002, doi:10.1029/2000RG000095.

Querol, X., M. Pandolfi, J. Pey, A. Alastuey, M. Cusack, N. Pérez, F. Amato, T. Moreno, M. Viana, and N. Mihalopoulos (2009), African dust contribution to mean ambient PM10 mass-level across the Mediterranean Basin, *Atmos. Environ.*, *43*, 4266–4277, doi:10.1016/j.atmosenv.2009.06.013.

Rodríguez, S., X. Querol, A. Alastuey, G. Kallos, and O. Kakaliagou (2001), Saharan dust contributions to PM10 and TSP levels in southern and eastern Spain, *Atmos. Environ.*, *35*, 2433–2447, doi:10.1016/S1352-2310(00)00496-9.

Rodríguez, S., A. Alastuey, S. Alonso-Perez, X. Querol, E. Cuevas, J. Abreu-Afonso, M. Viana, M. Pandolfi, and J. de la Rosa (2011), Transport of desert dust mixed with North African industrial pollutants in the subtropical Saharan Air Layer, *Atmos. Chem. Phys.*, *11*, 6663–6685, doi:10.5194/acp-11-6663-2011.

Santos, D., M. J. Costa, and A. M. Silva (2008), Direct SW aerosol radiative forcing over Portugal, *Atmos. Chem. Phys.*, *8*, 5771–5786, doi:10.5194/acp-8-5771-2008.

Schoeberl, M. R., et al. (2006), Overview of the EOS Aura Mission, *IEEE Trans. Geosci. Remote Sens.*, *44*, 1066–1074, doi:10.1109/TGRS.2005.861950.

Seckmeyer, G., A. F. Bais, G. Bernhard, M. Blumthaler, C. R. Booth, K. Lantz, R. L. McKenzie, P. Disterhoft, and A. Webb (1997), Instruments to measure solar ultraviolet radiation. Part 2: Broadband instruments measuring erythemally weighted solar irradiance, *WMO GAW, 164*, World Meteorol. Organ., Geneva, Switzerland.

Tanskanen, A., N. A. Krotkov, J. R. Herman, and A. Arola (2006), Surface ultraviolet irradiance from OMI, *IEEE Trans. Geosci. Remote Sens.*, *44*, 1267–1271, doi:10.1109/TGRS.2005.862203.

Tanskanen, A., et al. (2007), Validation of daily erythemal doses from OMI with ground-based UV measurement data, *J. Geophys. Res.*, *112*, D24S44, doi:10.1029/2007JD008830.

Toledano, C., V. E. Cachorro, A. M. de Frutos, M. Sorribas, N. Prats, and B. A. de la Morena (2007), Inventory of African desert dust events over the southwestern Iberian Peninsula in 2000–2005 with an AERONET Cimel Sun photometer, *J. Geophys. Res.*, *112*, D21201, doi:10.1029/2006JD008307.

Udo, S. (2000), Sky conditions at Ilorin as characterized by clearness index and relative sunshine, *Sol. Energy*, *69*, 45–53, doi:10.1016/S0038-092X(00)00008-6.

Valenzuela, A., F. J. Olmo, H. Lyamani, M. Antón, A. Quirantes, and L. Alados-Arboledas (2012a), Analysis of the desert dust radiative properties over Granada using principal plane sky radiances and spheroids retrieval procedure, *Atmos. Res.*, *104–105*, 292–301, doi:10.1016/j.atmosres.2011.11.005.

Valenzuela, A., F. J. Olmo, H. Lyamani, M. Antón, A. Quirantes, and L. Alados-Arboledas (2012b), Classification of aerosol radiative properties during African desert dust intrusions over southeastern Spain by sector origins and cluster analysis, *J. Geophys. Res.*, *117*, D06214, doi:10.1029/2011JD016885.

Vilaplana, J. M., et al. (2009), Report of the El Arenosillo/INTA-COST calibration an intercomparison campaign of UVER broadband radiometers, report, 64 pp., COST Off., Brussels.

Wagner, F., et al. (2009), Properties of dust aerosol particles transported to Portugal from the Sahara desert, *Tellus, Ser. B*, *61*, 297–306, doi:10.1111/j.1600-0889.2008.00393.x.

Webb, A., J. Gröbner, and M. Blumthaler (2006), A practical guide to operating broadband instruments measuring erythemally weighted irradiance, 21 pp., Off. for Off. Publ. of the Eur. Comm., Luxembourg.

Weihs, P., et al. (2008), Measurements of UV irradiance within the area of one satellite pixel, *Atmos. Chem. Phys.*, *8*, 5615–5626, doi:10.5194/acp-8-5615-2008.